Integrating an Islet-Based Biosensor in the Artificial Pancreas: In Silico Proof-of-Concept

Loïc Olçomendy, *Member, IEEE*, Antoine Pirog, Fanny Lebreton, Manon Jaffredo, Louis Cassany, David Gucik Derigny, Jérôme Cieslak, David Henry, Jochen Lang, Bogdan Catargi, Matthieu Raoux, Yannick Bornat, and Sylvie Renaud

Abstract*—*Objective: **Current treatment of type 1 diabetes by closed-loop therapy depends on continuous glucose monitoring. However, glucose readings alone are insufficient for an artificial pancreas to truthfully restore nutrient homeostasis where additional physiological regulators of insulin secretion play a considerable role. Previously, we have developed an electrophysiological biosensor of pancreatic islet activity, which integrates these additional regulators through electrical measurements. This work aims at investigating the performance of the biosensor in a blood glucose control loop as potential in silico proof-of-concept. *Methods:* Two islet algorithm models were identified on experimental data recorded with the biosensor. First, we validated electrical measurement as a means to exploit the inborn regulation capabilities of islets for intravenous glucose measurement and insulin infusion. Subsequently, an artificial pancreas integrating the islet-based biosensor was compared to standard treatment approaches using subcutaneous routes. The closed-loop simulations were performed in the UVA/Padova T1DM Simulator where a series of realistic meal scenarios were applied to virtual diabetic patients. *Results:* With intravenous routes, the endogenous islet algorithms successfully restored glucose homeostasis for all patient categories (mean time in range exceeds 90%) while mitigating the risk of adverse glycaemic events (mean BGI < 2). Using subcutaneous routes, the biosensor-based artificial pancreas was as efficient as standard treatments, and outperformed them under challenging conditions. *Conclusion:* This work validates the concept of using inborn pancreatic islets algorithms in an artificial pancreas in silico. *Significance:* Pancreatic islet endogenous algorithms obtained via an electrophysiological biosensor successfully regulate blood glucose levels of virtual type 1 diabetic patients.**

***Index Terms*—Artificial pancreas, biosensor, control algorithm, diabetes, MEA, UVA/padova T1DMS.**

I. Introduction

CONTINUOUS monitoring linked to drug delivery is a proven approach for the treatment of type 1 diabetes mellitus (T1D) and provides powerful means to improve therapeutic outcomes and the quality of patient's life [1]. Indeed, Continuous Glucose Monitoring (CGM) systems associated to insulin delivery (constituting an Artificial Pancreas or AP), have provided a major advance in assessing glucose variability at resolutions unattainable through traditionnal Self Monitoring of Blood Glucose (SMBG) or HbA1c measurement, thus enabling intensive glycaemic control [2].

CGM sensors use electrochemical electrodes to measure subcutaneous glucose as capillary glucose equilibrates in the interstitial fluid [3]. Patients then rely on the use of algorithms (either a bolus calculator or an AP controller) to adequately dose insulin delivery. However, the regulation process is currently limited by the nature of glucose-only sensors.

The predictive power and robustness of current single input control algorithms do not suffice to cope with real world variability especially in a pathological setting [4]. Indeed, latest AP control algorithms only account for one physiological metric (glucose), and rely on additional patient-provided inputs (e.g., meal announcement, physical exercise announcement) to achieve best performance. Such hybrid closed-loop systems (e.g., Minimed 670G, Control-IQ) have been approved in the US and in Europe [5]. They partially automate insulin delivery, with meal boluses still requiring patient intervention.

In contrast to current CGM devices, pancreatic islets are the "in-born" sensors and actuators, optimally shaped during 0.5 billion years of evolution to integrate the prevailing physiological situation [6]. Indeed, glucose but also lipids, amino acids and a number of important signals (mostly hormonal), are integrated by the endogenous algorithms thus providing, information on the general body status and the ensuing metabolic requirements as during stress or physical activity [7]. Moreover, islets contain not only insulin-secreting β-cells, but also other endocrine cells

Manuscript received February 19, 2021; revised May 27, 2021 and July 23, 2021; accepted July 26, 2021. Date of publication September 1, 2021; date of current version January 20, 2022. This work was supported in part by the Fonds Européen de Développement Régional (FEDER) under Grant Agreement DIAGLYC No. 3538519 and in part by the French Agence Nationale de la Recherche (ANR) under Grant Agreement DIABLO No. ANR-18-CE17-0005-01. *(Corresponding author: Loïc Olçomendy.)*

Loïc Olçomendy is with the Université de Bordeaux, CNRS, Bordeaux INP, IMS, UMR 5218, F-33400 Talence, France (e-mail: loic.olcomendy@ims-bordeaux.fr).

Antoine Pirog, Louis Cassany, David Gucik Derigny, Jérôme Cieslak, David Henry, Yannick Bornat, and Sylvie Renaud are with the Université de Bordeaux, CNRS, Bordeaux INP, IMS, France.

Fanny Lebreton is with the Université de Bordeaux, CNRS, Bordeaux INP, CBMN, UMR 5248, France, and also with the Cell Isolation and Transplantation Center, Surgery, Hospitals and University of Geneva, Switzerland.

Manon Jaffredo, Jochen Lang, and Matthieu Raoux are with the Université de Bordeaux, CNRS, Bordeaux INP, CBMN, France.

Bogdan Catargi is with the Bordeaux Hospitals, Diabetology Unit, France.

Digital Object Identifier 10.1109/TBME.2021.3109096

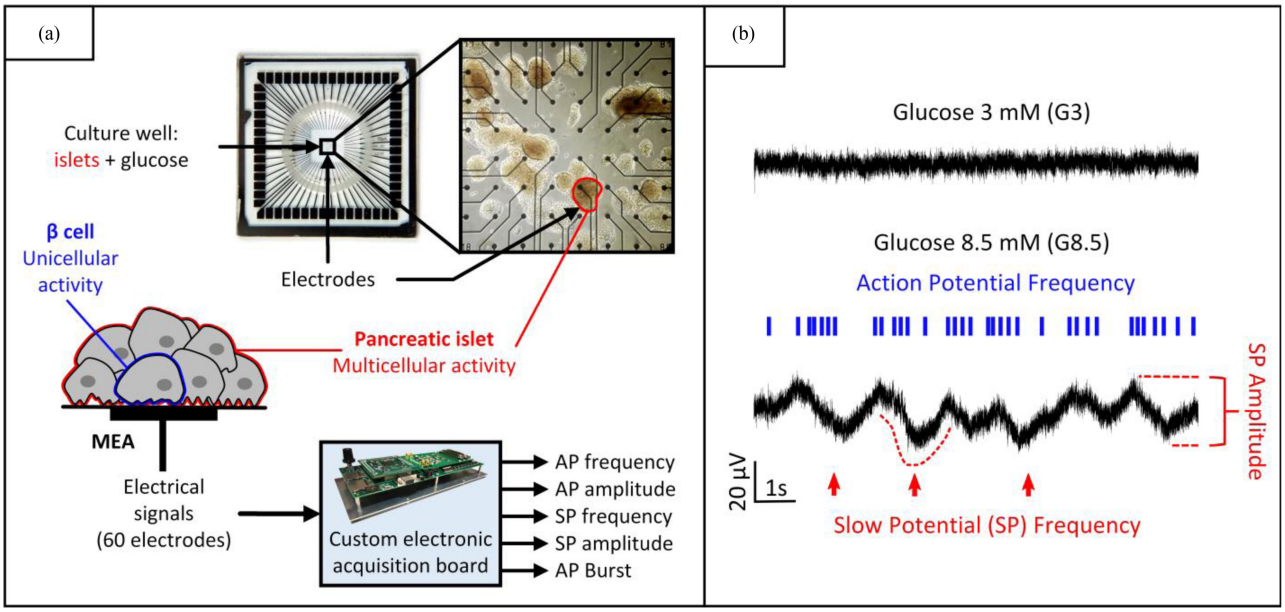

Fig. 1. Biosensor principle: acquisition and processing of electrical biosignals generated by pancreatic islets cultured on MEAs and subjected to glucose. (a) Pancreatic islets cultured on MEAs. Glucose can be introduced in the culture chamber to stimulate the cells. Each electrode in the MEA captures a combination of uni- and multicellular activity in the neighbouring islets. A custom electronic board performs online digital signal processing on the recorded biosignals to extract features of interest for each electrode. (b) Measured electrical activity is modulated by glucose concentration (unpublished data recorded during the study in Lebreton *et al.*, 2015). Low glucose inhibits activity and high glucose induces two signals of interest, representative of uni- and multicellular activity: action potentials and SPs. Action potentials are mainly characterized by their frequency, and SPs by both their frequency and amplitude.

such as α, δ, or γ, and their local interactions shape further the physiological response [8]. Islets also encode physiologically important kinetics such as biphasic insulin secretion [9], which is best for insulin action, and glucose-dependent hysteresis protecting from hypoglycaemia [10], [11]. Islets, composed of up to a thousand excitable cells, display continuous ionic current oscillations upon activation, which are measurable as an electrical signal and are shaped by the endogenous islet algorithms.

We have designed and patented a novel hybrid biosensor (see Fig. 1) that benefits from the natural sensing features of islets: this sensor is based on a Micro-Electrode Array (MEA) which measures, on up to 60 recording sites, the extracellular electrical activity of a few murine or human islets and is linked to real-time/online signal processing [12]. The resulting electrical signals integrate the action of all the mediators of insulin secretion. This sensor module (see Fig. 1A) is currently used in a clinical study for in vitro quality control of human donor islets prior to transplantation [13].

The biosensor measures extracellular field potentials, so called Slow Potentials (SPs), induced by nutrients and regulated further by hormones. While action potentials are generated at the single-cell level, SPs, like local field potentials in neurons, are multicellular oscillatory events resulting from complex temporal and spatial summations of ion fluxes (see an illustration in Fig. 1B). These signal components are processed for feature extraction by our acquisition system (see Fig. 1A). Among the several features computed, the frequency of SPs reflects in the most faithful manner the whole islet activity, involving intercellular coupling, a crucial parameter for proper insulin release [14]. It ranges between [0.2; 2.0] Hz, and is robustly measured thanks to the large signal-to-noise ratio of SPs [11]. The biosensor therefore serves as a proxy for islet endogenous algorithms which are responsible for insulin secretion dynamics.

Simulation of metabolic processes has a recognised clinical relevance in developing solutions for the treatment of diabetes [15]. Simulations offer the possibility to perform extensive tests with significant time and cost savings, not to speak of ethical aspects. Based on a comprehensive mathematical model of the glucose-insulin dynamics and equipped with a population of virtual T1D patients, the UVA/Padova Type 1 Diabetes Mellitus Simulator (T1DMS) is a renowned and commercially-available testing environment for glucose sensors, control algorithms, and pumps involved in modern T1D therapy. Accepted by the U.S. Food and Drug Administration as a substitute for pre-clinical animal trials [16], [17], the T1DMS is widely used in the AP community to tune and validate closed-loop insulin infusion strategies [18]–[20]. Since the latest commercial version, the simulator was upgraded to account for intra- and inter-subject variabilities of insulin sensitivity throughout the day, thus enabling the realistic simulation of multi-meal scenarios. The updated model equations, described in Visentin *et al.* [21], are not integrated in the commercial version, and model parameters have not been released.

Our study aims at investigating the relevance of an extracorporeal islet-based biosensor, as well as its capacity to perform in an AP configuration. We hypothesized that, in contact with T1D patient interstitial fluids, healthy islets embedded in our extracorporeal biosensor could provide an indication on the patient's need in insulin and thus constitute a valuable physiological input for the AP. Specifically designed

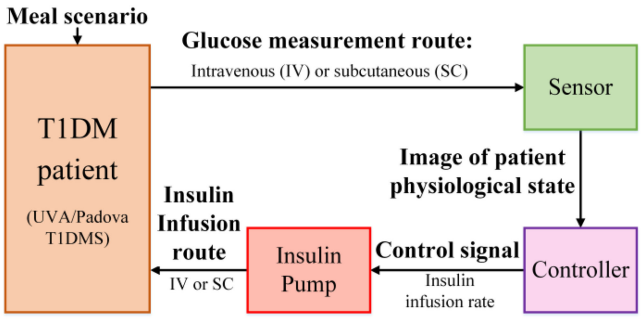

Fig. 2. Artificial Pancreas (AP) in silico testing environment. A T1D patient model receives insulin input from an insulin pump. The insulin infusion rate control algorithm is computed by a controller that receives the patient glucose measurements through a sensor.

for the testing of AP systems, the T1DMS therefore appears as a relevant tool to evaluate our biosensor as part of a Blood Glucose (BG) regulation closed loop.

The biosensor's conjectured added value comes from its sensitivity to all initiators and modulators of endogenous insulin secretion. As a starting point, glucose levels will be the only input of the biosensor in this study. This limitation also stems from the current absence of a commercial simulator capable of modelling the variation of insulin secretion regulators other than glucose (e.g., fatty acids, amino acids, hormones).

In this study, we propose two data-based biosensor models of the non-bijective dynamic response to rising/decreasing glucose. Using the T1DMS as an in silico testing environment for our AP, i.e., a model of our biosensor, a control algorithm and an insulin pump model, we tuned controllers individually to fulfill each patient's needs, and the resulting AP was then tested with realistic meal scenarios. In a configuration where glucose level was the only available input for the biosensor, we compared our AP to other standard insulin delivery techniques in realistic meal scenarios. With this approach, we aimed at providing a first assessment of the closed-loop performance of our biosensor-based AP.

II. Methods

A. In Silico Testing Environment

1) Simulation Principle: The latest commercial version of the T1DMS (The Epsilon Group, version 3.2) was used for the simulations. The T1DMS provides CGM sensor and insulin pump models, as well as a metabolic model of T1D patients. The latter simulates the glucose-insulin interactions in virtual T1D patients subjected to glucose intake scenarios with physiological accuracy. It takes the meal (glucose intake) scenario and the insulin infusion rate as inputs, and provides as output the patient's glucose concentrations following the equations described in Dalla Man *et al.* [22]. For the AP controller, the variables of interest are glucose (either intravenous or subcutaneous concentration) and insulin (also intravenous or subcutaneous - see Fig. 2). Meal scenarios are user-defined and set the timing and levels of glucose ingestions. The simulator also provides a built-in meal anouncement feature to simulate the interactions between the patient and the control algorithm.

2) T1DMS Configuration: Our work is based on simulation data obtained with two different configurations of the T1DMS. The first one used the intravenous (IV) glycaemia measurement and insulin delivery routes and will be referred to as IV/IV configuration. With this configuration, our objective was to validate the SP frequency signal as a relevant indicator of insulin need. The insulin infusion signal was therefore generated using a model of SP frequency variations. When the model is connected to the simulator using IV measurement and IV insulin infusion routes (no insulin pump in the loop – see Fig. 5A), the insulin regulation is performed without diffusion delays (as would be the case with the healthy endocrine pancreas). This configuration was used as a proof-of-concept to evaluate the electrically-characterised endogenous islet algorithms alone, without any error compensation from a controller. This configuration emphasizes the inborn regulation capabilities of pancreatic islets.

The second configuration used the subcutaneous (SC) insulin delivery route as it is systematically used to ensure patient safety in actual T1D therapy. Islets are now considered as embedded in an extracorporeal implementation of the biosensor and fed with patient's subcutaneous fluid. This configuration will therefore be referred to as SC/SC. T1DMS configured in SC/SC simulates an AP with a sensor and a pump (both extracorporeal) which is the reference therapy for T1D patients. The main difference with IV/IV configuration is the presence of delays resulting from glucose diffusion in the SC space and from SC insulin absorption. We used the T1DMS in SC/SC configuration to simulate, as best as the software currently allows, the everyday life of patients by pairing it to realistic glucose intake scenarios when assessing the capacity of our biosensor to regulate the patients' BG level.

B. Islet Algorithms Model Identification

The experimental data for the model extraction were recorded as described in Lebreton *et al.* [11]. Mouse islets were subjected to a series of ascending, then descending glucose concentrations. Signals were filtered using a Butterworth 0.2-2.0 Hz filter, and SP events were detected using the algorithm presented in Pirog *et al.* [23]. The average frequency of those events was calculated, and normalized, at steady state during the last 3–7 min of each glucose condition.

Two models were identified from the normalized glucose-dependent SP frequency. As a first step, a static model was identified using the method of least squares solved by the Trusted Region Reflective algorithm (using scipy.optimize's curve_fit function). Though this model does not account for the asymmetry of the glucose response, it was used as a computationally inexpensive solution.

Given the asymmetrical response measured [11], a hysteretic model was then identified using a discrete Preisach model [24], which decomposes hysteretic phenomena as a summation of elementary relay hysterons distributed on the so-called Preisach plane. To avoid propagation of measurement errors within the model, experimental data were split between increasing and

decreasing glucose conditions, and fitted to two separate static models using the method described above. The region between the two resulting curves was then utilized to compute the weights of the relay hysterons and establish the model.

Identification of the static model was initially performed in Python 2.7 and the resulting model was subsequently translated in Matlab to satisfy compatibility with the T1DMS. Likewise, and for the same reasons, the Preisach model was initially identified in Python 2.7 with an algorithm adapted from Janičić *et al.* [25], then translated into Matlab.

In addition to the T1DMS proprietary metabolic model, we used three components for these configurations: i) sensor models; ii) controllers (both described below); iii) the default insulin pump model from the T1DMS component library.

C. Control Algorithms

1) An Unconventional Sensor: Control algorithms are a key component in AP systems and thus received much attention in biomedical research. However, as this work is not focused on control theory and for the sake of demonstration, we used simple Proportional-Integral-Derivative (PID) controllers to handle the subcutaneous diffusion delays induced by the SC/SC configuration. It is important to note the unconventional nature of the biosensor in this work. The output of the biosensor is an image of electrical islet activity and integrates the action of all the regulators of insulin secretion as well as physiologically important intra-islet regulations [8]. It thus provides an image of the patient's physiological state (see Fig. 2) and represents an insulin demand signal rather than a glucose level signal. In the healthy individual, islets act as the natural sensor, control algorithm and actuator that enable glucose homeostasis. Monitoring their electrical activity therefore amounts to monitoring the natural control algorithm output. As a consequence, the output of the biosensor is intrinsically compared to 0 (no insulin need) due to the endogenous algorithms of pancreatic islets generating the SP frequency. This characteristic has thus the advantage of avoiding the use of a personalized setpoint to guarantee an efficient BG regulation.

2) Controller Architecture: The controller of an AP determines the appropriate quantity of insulin to be delivered in response to significant disturbances, such as a meal or physical effort. To that avail, the controller takes into account present and past sensor readings, but also anticipates the future states determined by glucose-insulin interactions and insulin onset of action.

In the IV/IV configuration, a controller is not needed and the insulin infusion rate is directly derived from the biosensor output. The insulin command law is qualitatively adapted to the patients prevailing physiological state by the islet's algorithms. A simple gain is then used to quantitatively adapt the insulin need signal: the resulting insulin infusion rate is proportional to the sensor output, by a factor K optimized to match the need of insulin for each patient. The endocrine pancreas of the patient is then replaced by the islet algorithm model in series with the gain K (in pmol/min/Hz).

In the SC/SC configuration (i.e., the "standard" AP configuration), a controller is necessary to handle the delays induced by subcutaneous glucose measurement and subcutaneous insulin infusion. The controller also guarantees the stability of the closed-loop system.

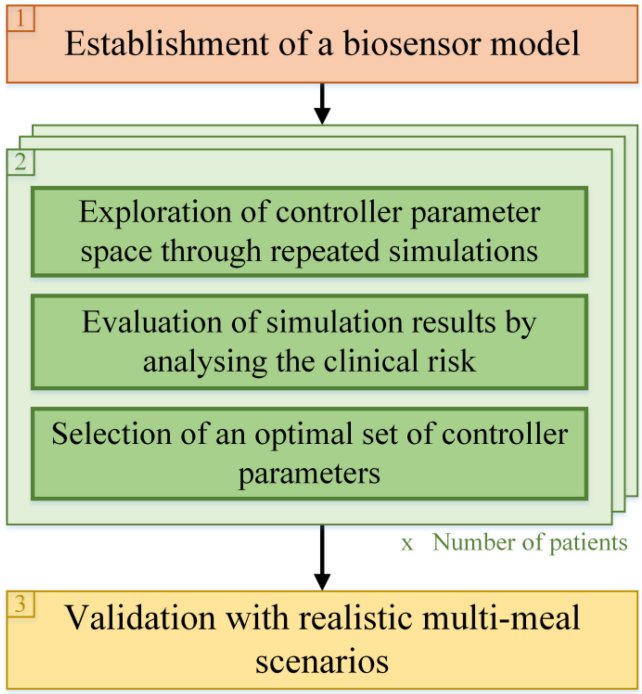

Fig. 3. Control algorithm design flow: using a pre-defined biosensor model (1), the controller parameters are individually tuned through an automated GA-based process which explores the parameters space and assesses their performance by analysing simulation results, and finally selects an optimal set of parameters that minimizes a glycaemia-related clinical risk marker (BGI) (2). The diabetic patient cohort is then submitted to a validation multi-meal scenario (3).

3) Controller Tuning: In the AP development process, the large inter-patient variability in terms of sensitivity to insulin, body weight, and T1D duration is a serious issue in designing easily adjustable devices. The amount of insulin required to normalize BG levels after a meal greatly varies among patients. To account for this variability as well as to ensure reliability and stability of the closed-loop system, a fine tuning of the AP controller's parameters is necessary.

To achieve this goal, we developed an in silico tuning method based on a Genetic Algorithm (GA, see Fig. 3). It is used together with a cost function that computes the mean Blood Glucose Index (BGI - further described in the next section) of BG profiles resulting from single meal simulations. This algorithm optimizes controllers that minimize the clinical risk associated with the patient's glycaemia. This tuning method is further detailed in Olçomendy *et al.* [26] with a minor difference: the fmincon function is no longer used to select the optimal parameters of the controller. Instead, we compute average parameters with the 10 best controllers provided by the GA. This eliminates an unfair disadvantage induced by fmincon when it comes to tuning controllers paired with noisy CGM sensors.

A PID controller was tuned with this method for each adult of the UVA/Padova T1D cohort. For comparison, the same method was also used to tune PID controllers coupled with the T1DMS's default CGM sensor. Ultimately, the Multiple Daily

Injections (MDI) therapy was used as a third comparison. This built-in feature of the T1DMS is implemented with optimal basal insulin infusion rate and carbohydrates ratio provided for all patients of the cohort. When specified, the method published by Herrero *et al.* [18] was implemented in simulations involving MDI - to model the reported errors in carbohydrate counting by patients (ranging from -30% to +40%). The Biosensor-based AP (Biosensor-AP) overall performance was then compared to the CGM-based AP (CGM-AP) and the MDI therapy in a series of realistic unannounced meal scenarios simulated on the adult population of the T1DMS.

D. Analysis Tools and Performance Assessment Metrics

The considerable progress and increased popularity of CGM [1] came with a need for standardization of performance metrics in both closed- and open-loop insulin therapies. To this end, recommendations regarding CGM metrics were formulated in 2017 [27]–[29]. At the 2019 Advanced Technologies & Treatments for Diabetes (ATTD) annual congress, a panel of international CGM technologies experts agreed on these metrics and defined their clinical targets for different diabetes populations. The consensus was published and endorsed by several diabetes professional associations such as ADA and EASD [30]. We selected eight of the recommended metrics (and their associated targets), detailed below, to assess the performances of our Biosensor-AP:

- *Mean Glucose:* mean glucose is a common performance indicator of insulin delivery therapies. Traditionally, the mean BG over the past few months was estimated through HbA1C measurement, which is still a 'gold-standard', yet estimation with CGM datasets is now favoured for its greater resolution.
- *Time In Range (TIR):* time spent in a given range by the glycaemia of a patient is a widely used indicator to assess performance of APs. TIR refers to the time spent in normoglycaemia (70 to 180 mg/dl; 3.9 to 10 mmol/dl). TIR is more sensitive to acute hypo- or hyperglycaemia events than HbA1C and is generally preferred to other metrics thanks to its straightforward meaning for real-life diabetology.
- *Time Below Range (TBR 1 and TBR 2):* the time spent below a given BG level. The first considered level is 70 mg/dl (3.9 mmol/dl; TBR 1) and the second is 54 mg/dl (3.0 mmol/dl; TBR 2).
- *Time Above Range (TAR 1 and TAR 2):* the time spent above a given BG level. The first considered level is 180 mg/dl (10 mmol/dl; TAR 1) and the second is 250 mg/dl (13.9 mmol/dl; TAR 2).

As T1DMS does not label "high risk patients" (according to the nomenclature used in Battelino *et al.*[30]) in its cohort, we therefore considered that the whole cohort was constituted of "normal" T1D patients. The simulation results were therefore compared to the targets below, recommended for this diabetes population[30]: TBR 2 $<$ 1%, TBR 1 $<$ 4%, TIR $>$ 70%, TAR 1 $<$ 25%, and TAR 2 $<$ 5%.

We also used the Blood Glucose Index (BGI) described in Kovatchev *et al.* [31] as a clinically-relevant performance indicator to tune the AP controller, following the method we described in Olçomendy *et al.* [26] and for performance analysis. The BGI provides a symmetrical metric to handle the asymmetric risk distribution around the patient target BG (elevated glucose levels can be tolerated by a patient for some time, whereas hypoglycaemia quickly becomes life-threatening). In 2005, Kovatchev *et al.* [31] also introduced two other metrics derived from BGI:

- *Low BGI (LBGI):* This metric is a measure of the frequency and extent of low BG readings and has been validated as an excellent predicator of severe hypoglycaemic events.[32] The T1DMS User Guide indicates that LBGI is considered minimal when lower than 1.1, low ($1.1 \leq \text{LBGI} < 2.5$), moderate ($2.5 \leq \text{LBGI} < 5$), and high when higher than 5.0.
- *High BGI (HBGI):* This metric is a measure of the frequency and extent of high BG readings and showed reliable performances in predicting risk for hyperglycaemia [32]. HBGI is considered minimal when lower than 5.0, low ($5.0 \leq \text{HBGI} < 10.0$), moderate ($10.0 \leq \text{HBGI} < 15$), and high when higher than 15.0.

In addition, we systematically computed the Total Daily Insulin (TDI) for performance analysis during both development and validation phases. There are neither official recommendations nor targets concerning the TDI infusion for T1D patients because insulin needs vary greatly across the patient population according to their diet, physical activity or their own physiological characteristics. However, TDI still is an interesting indicator to objectively compare different regulation strategies. It is also useful to detect deficient or excessive aggressiveness in the tuning of the controller.

To complete the performance analysis, normality was tested using the Shapiro-Wilk test and statistical significance was then assessed using either the two-sided paired sample t-test or the two-sided Wilcoxon signed rank test. P-values lower than 0.01 were considered significant.

E. Glucose Intake Scenarios

The meal scenarios being investigated are two realistic 48-hour multi-meal scenarios which match the average daily carbohydrates intake observed in adult T1D patients (in the USA) [33].

One scenario consists of a 3-meal/2-snack daily pattern in which a total of 235 g of glucose is ingested each day. The meals are distributed as follows: a breakfast of 45 g of glucose ingested at 6 a.m., a lunch of 70 g at noon and a dinner of 80 g at 6 p.m. Two 20 g snacks are added at 4 p.m. and 11 p.m.

The other scenario consists of a more challenging 2-meal/1-snack pattern in which a total of 240 g of glucose is ingested each day. The meals are distributed as follows: a large brunch of 100 g of glucose ingested at 10 a.m. and a large dinner of 120 g at 8 p.m. A 20 g snack is added at 5 p.m.

For both scenarios, the same glucose intake pattern was repeated on two consecutive days in order to assess the daily BG profile stability. In the results section, the considered glucose profiles correspond to the second day of each scenario. In this

TABLE I
MODEL PARAMETERS FOR STATIC AND HYSTERETIC MODELS, AND CORRESPONDING COEFFICIENT OF DETERMINATION R^2. RESULTS ARE VALUE (STANDARD ERROR)

Parameter	Static model	Hysteretic model		Unit
		Upper envelope	Lower envelope	
G_0	2.0164 (21.5693)	5.3595 (0.5640)	5.6991 (2.2138)	mM
G_{50}	8.9334 (1.7512)	7.9733 (0.1036)	9.6062 (0.0964)	mM
n	5.8934 (23.5199)	2.1880 (0.5418)	4.2883 (2.6972)	.
f_M	0.4867 (0.3388)	0.4921 (0.1001)		Hz
R^2	0.8317	0.9859	0.9790	

way, the initial transition phase is excluded from the dataset used for the performance analysis.

When several repetitions of the glucose intake scenario are simulated to average out randomised behaviors (e.g., CGM noise [34], errors in carbohydrate counting), we consider that a patient has globally reached the recommended targets [30] if the regulation allows this patient to effectively reach these targets in more than 90% of the scenario repetitions (e.g., at least 23 out of 25 repetitions).

III. RESULTS

A. Islet Algorithms Models

1) Static Model: The Hill equation [35], widely utilized to represent biological processes, was chosen to model the islet response to glucose stimulation measured by the biosensor [11].

It is assumed that the concentration of glucose has to exceed a threshold to affect islet activity. Hence, we defined an activation function for glucose, modelled as :

$$\mathcal{A}\ (G) = \begin{cases} \dfrac{[G-G_0]^n}{[G_{50}-G_0]^n - [G-G_0]^n} & \text{if } G \geq G_0 \\ 0 & \text{otherwise} \end{cases} \quad (1)$$

Where G is the concentration of glucose, G_0 is the glucose threshold concentration, G_{50} is the half maximal effective glucose concentration, and n is the Hill coefficient. Islet activity is maximal when $\mathcal{A} = 1$ and null when $\mathcal{A} = 0$.

The activation function is then scaled by a factor f_M to obtain the islet SP frequency :

$$f\ (G) = f_M \times \mathcal{A}\,(G) \quad (2)$$

Equations (1–2) define the static model. Experimental conditions, identification results (parameters, goodness of fit) and model behaviour are presented in Fig. 4 and Table I.

2) Hysteretic Model: The hysteretic model is defined by its envelope, which upper and lower parts were fitted to two distinct static models on experimental conditions with respectively increasing and decreasing glucose concentrations. To ensure continuity between both parts at large values of G, a single parameter f_M was computed: f_M was identified for the upper envelope, and was forced to the same value for the lower envelope. Continuity in sub-threshold glucose concentrations is automatically ensured as long as $G_0 > 0$. Again, identified parameters and goodness of fit are presented in Table I. With the upper and lower envelopes identified, the weights of a 300×300 grid of uniformly distributed relay hysterons were computed according to the method described in Janičić *et al.* [25]. Resulting model behaviour can be seen in Fig. 4A-B.

Predictably, R-squared measure of goodness of fit as well as parameter standard error highlight the better modelling of the experimental data yielded by the hysteretic model as compared to the static model (0.82 vs 0.98).

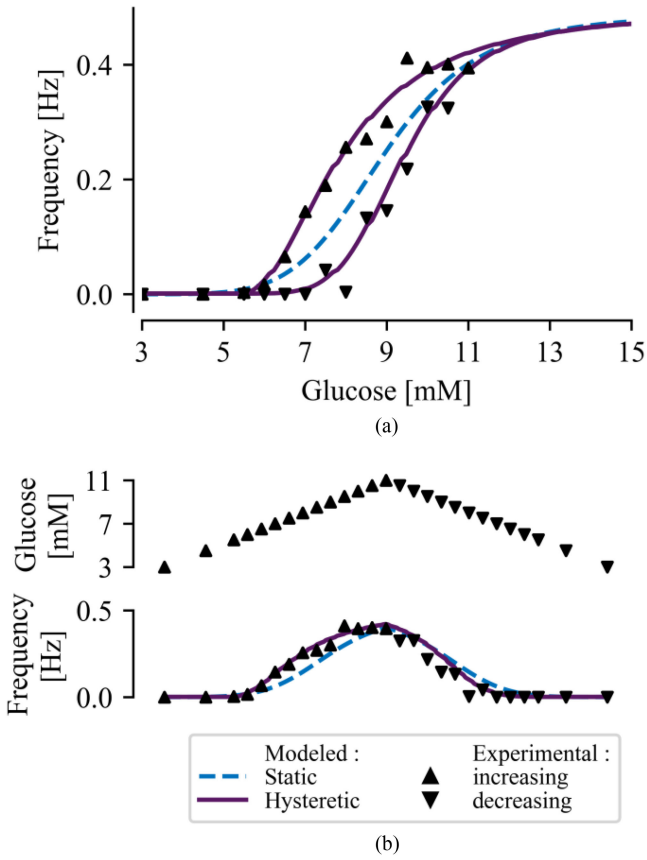

Fig. 4. Identified static and hysteretic models superimposed with experimental data. Experimental conditions with increasing or decreasing glucose concentrations are marked with appropriately directed triangles. Each step of the glucose ramps lasted 7 min. (a) Glucose-dependent modelled frequency response in increasing and decreasing glucose conditions. (b) *Sequential* view of modelled frequency response to glucose.

TABLE II
PERFORMANCE METRICS FOR DIFFERENT REGULATION SCHEMES IN ALL THREE PATIENT CATEGORIES

Category		TIR (%)	BGI (.)	TDI (U)
Adu.	Stat.	99.3 (1.1)	0.7 (0.2)	53.1 (13.1)
	Hyst.	99.8 (0.4)	0.6 (0.1)	54.3 (14.5)
Ado.	Stat.	94.5 (6.6)	1.5 (1.4)	42.1 (11.7)
	Hyst.	95.8 (5.4)†	1.2 (1.0)†	44.0 (13.3)
Chi.	Stat.	92.7 (3.5)	1.9 (0.9)	26.1 (7.4)
	Hyst.	92.6 (2.7)	1.9 (0.5)	25.4 (7.6)

Simulation results were analysed for adults (Adu.), adolescents (Ado.), and Children (Chi.) after closed-loop simulations with static (Stat.) and hysteresic (Hyst.) regulation schemes. The metrics extracted for this comparison are the Time In Range (TIR) percentage, Blood Glucose Index (BGI) (unitless), and Total Daily Insulin (TDI) units injected. All metrics are mean (SD). Symbol † indicates statistical significance ($p<0.01$) with respect to Stat.

B. Simulation Campaign

1) IV/IV Configuration: The pancreatic islet inner regulation capabilities were first assessed in IV/IV configuration (Fig. 5.A). Insulin infusion rate is controlled by a patient-adjusted proportional factor K. Both islet endogenous algorithm models were tested with the 2-day 3-meal/2-snack scenario (described in Methods section) on every patient (i.e., 11 adolescents, 11 adults, and 11 children). The mean BG profiles for each modality (averaged over the 11 patients of each population) are presented in Fig. 5.B.

Performance was assessed by calculating the mean TIR, mean BGI, and mean TDI (see Methods section) for each patient category (Adults, Adolescents, Children) and each regulation scheme (Static and Hysteresis). Results are summarized in Table II.

The regulation schemes based on islet endogenous algorithms (Static and Hysteretic models) ensured excellent performance of the BG regulation closed-loop. The mean TIR was above 90% for all patient categories and very close to 100% for adults. The biosensor algorithms maintain the BG level in the normoglycaemic range during the major part of the simulation with a very low risk of extreme glycaemic events (mean BGI < 2 in all patient categories), thus successfully restoring the glucose homeostasis of the patient. Concerning the mean TIR, IV/IV results showed a consistent trend in favour of the hysteretic model. This trend is statistically significant for adolescents ($p = 0.010$) but is not for adults and children (respectively $p = 0.098$ and $p = 0.492$). This led us to choose that model for the test of the in silico AP in an SC/SC configuration.

2) SC/SC Configuration: With SC glucose measurement and insulin infusion routes (Fig. 6.A), the T1DMS was exploited, in a more realistic configuration to compare our Biosensor-AP with two standard insulin therapy paradigms: MDI and a CGM-AP. We ran three case studies to assess their performance and robustness in realistic conditions of T1D patient's daily life. For each case study, the mean BG profile of the 11 adults is presented in Fig. 6B.

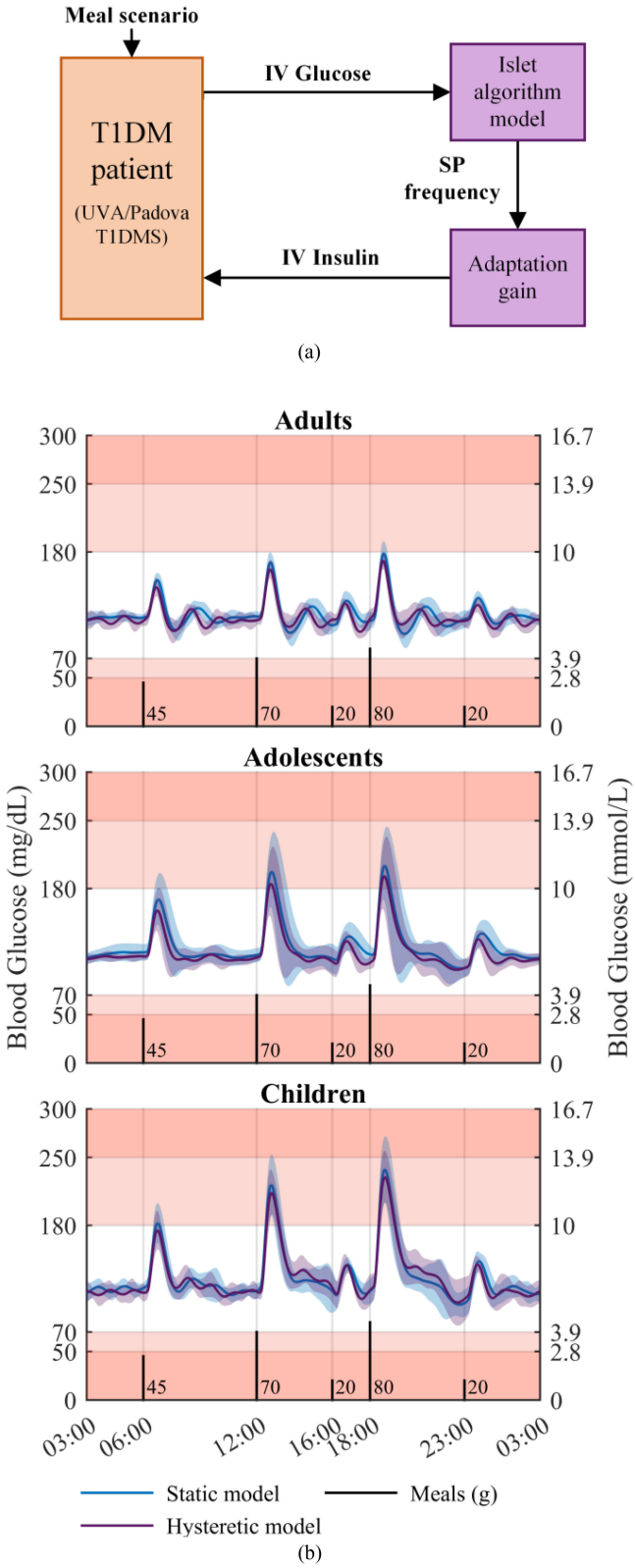

Fig. 5. (a) Islet-based regulation scheme using IV/IV configuration. (b) Simulation results for a 48-hour, 5-meal scenario (last 24 hours are displayed) in adults, adolescents, and children, for two regulation schemes (Static model, Hysteretic model) using IV glucose measurement and insulin infusion routes. Mean glucose profile (curve) and standard deviation (coloured patches) are displayed. Regions with no glycaemic risk, moderate glycaemic risk and high glycaemic risk are color-coded, respectively in white, *pink* and red.

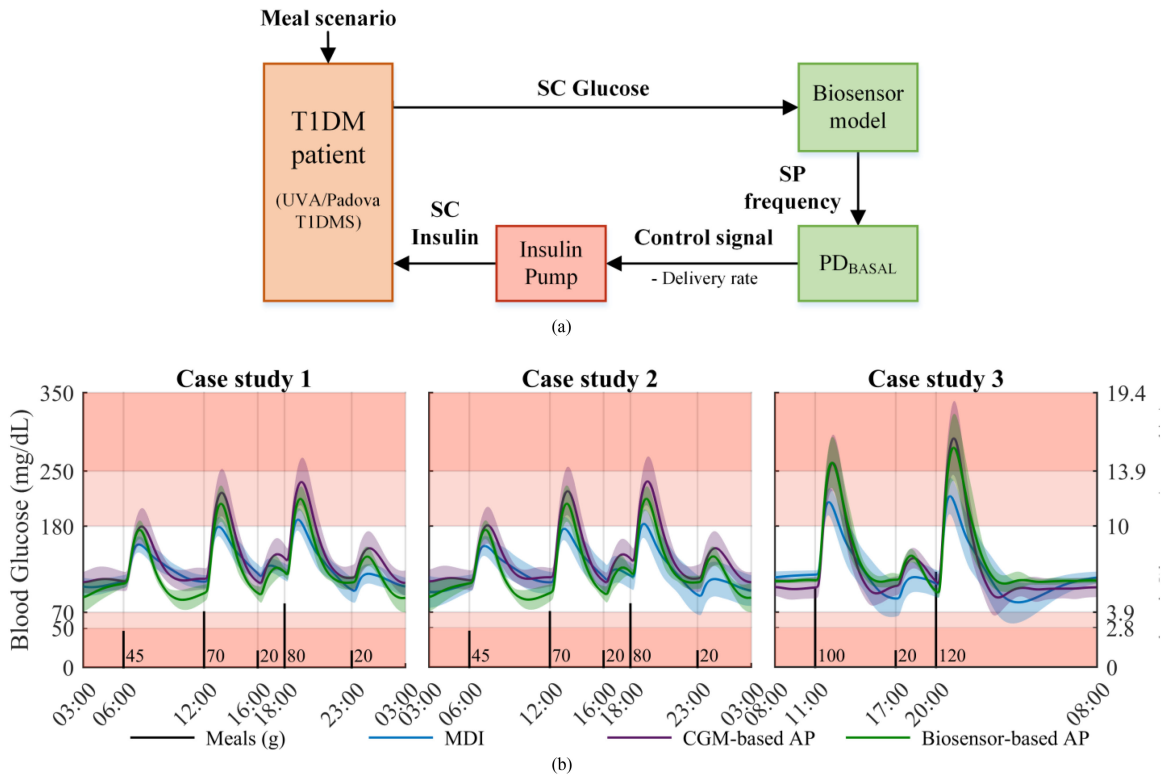

Fig. 6. (a) Biosensor-AP regulation scheme in SC/SC configuration. (b) Simulation results for three realistic 48-hour multi-meal scenarios in adults (last 24 hours are displayed), for three regulation schemes (Multiple Daily Injections (MDI), CGM-AP, Biosensor-based AP) using SC glucose measurement and insulin delivery routes. Mean glucose profile (curve) and standard deviation (coloured patches) are displayed. Regions with no glycaemic risk, moderate glycaemic risk and high glycaemic risk are color-coded, respectively in white, pink and red.

The first case study used the same 3-meal/2-snack scenario as the IV/IV closed-loop configuration. For case study 1, both the CGM-AP and the Biosensor-AP allowed 9 adults to reach the recommended targets. With the Biosensor-AP, the mean TIR presented a significant increase of 4.4% in the adult population (compared to CGM-AP) with a mean BGI[1] reduction of 0.9 (2.7 vs 3.6). Mean LBGI and HBGI of adults are minimal for both CGM- and Biosensor-APs and the mean glucose level is respectively equivalent to a mean HbA1C level of 6.6% and 6.4%.[2] MDI therapy showed excellent results with all the adults (11) reaching the targets with a mean BGI of 1.7. Detailed results are presented in Table III.

The second case study used the same meal scenario, but included realistic errors in carbohydrate counting. That scenario was used to quantify the impact of meal announcement accuracy, on which relies the top-of-the-art performance of the MDI therapy observed with scenario 1. A drop in the performance achieved by the MDI therapy was observed with only 5 adults reaching the targets (11 in case study 1) and a mean LBGI increasing from 0.2 to 0.8. That result highlights the crucial dependency of MDI on accurate meal announcement. As there are no meal announcements in the CGM- and Biosensor-APs, their performance indicators are identical to the ones from case study 1.

The third case study used the challenging 2-meal/1-snack scenario (described in Methods section). The MDI therapy (with random errors) and CGM-AP failed to maintain the patients in the targets; however, the Biosensor-AP allowed 4 adults to reach the targets, and kept both LBGI and HBGI minimal for all adults except adult#007.

IV. Discussion

Pancreatic beta cell activity is regulated through different pathways involving nutrients (glucose, FFAs, amino acids) and hormones (e.g., GLP-1, GIP, and adrenaline), and can be modulated with various drugs [7]. These molecules can be seen as the inputs of integrative endogenous algorithms which provide electrical activity and insulin secretion rate as outputs. Islet electrical responses to some of these insulin secretion regulators was experimentally studied with our biosensor and the tight correlation of electrical activity to secretion has been validated [9], [11], [12], [36].

As opposed to glucose-only CGM technologies, this multi-input islet-based biosensor would give new insights on the physiological status of T1D patients. Indeed, the embedded islets integrate information about nutrients and hormones in a single signal. Although the dynamics of islet response are shaped by the endogenous algorithms specifically for insulin release in the portal vein (intravenous route), we hypothesize that the biosensor can provide more reliable information than

[1]BGI = LBGI + HBGI (defined in Kovatchev *et al.*[31])

[2]The conversion was computed using the online eAG/A1C Conversion Calculator provided by the American Diabetes Association.

TABLE III
PERFORMANCE METRICS FOR DIFFERENT REGULATION SCHEMES IN THREE CASE STUDIES, FOR ALL ADULTS

Case study 1

Category		TBR 2 (%)	TBR 1 (%)	TIR (%)	TAR 1 (%)	TAR 2 (%)	LBGI (.)	HBGI (.)	Mean BG (mg/dl)	TDI (U)
Adu.	MDI	0.0 (0.0)	0.0 (0.0)	95.3 (4.1)	4.7 (4.1)	0.0 (0.0)	0.2 (0.2)	1.5 (0.7)	127.7 (9.2)	91.1 (20.7)
	CGM	0.1 (0.7)	0.4 (1.5)*	83.7 (7.3)*	15.9 (7.2)*	1.4 (3.1)	0.2 (0.4)	3.4 (1.6)*	140.5 (11.6)*	86.8 (19.1)
	Bios.	0.0 (0.0)	1.6 (3.2)	88.1 (5.4)*†	10.3 (3.4)*†	0.2 (0.7)	0.7 (0.6)	2.0 (0.7)†	124.4 (4.3)†	92.8 (21.7)†

Case study 2

Category		TBR 2 (%)	TBR 1 (%)	TIR (%)	TAR 1 (%)	TAR 2 (%)	LBGI (.)	HBGI (.)	Mean BG (mg/dl)	TDI (U)
Adu.	MDI	0.7 (2.4)	2.9 (5.6)	93.0 (7.1)	4.2 (4.9)	0.0 (0.0)	0.8 (1.1)	1.5 (0.9)	123.5 (11.5)	92.6 (20.3)
	CGM	0.0 (0.3)	0.1 (0.8)*	83.7 (7.3)*	16.1 (7.3)*	1.5 (3.3)	0.1 (0.2)*	3.4 (1.7)*	141.1 (12.0)*	86.7 (19.0)*
	Bios.	0.0 (0.0)	1.6 (3.2)	88.1 (5.4)*†	10.3 (3.4)*†	0.2 (0.7)	0.7 (0.6)†	2.0 (0.7)*†	124.4 (4.3)†	92.8 (21.7)†

Case study 3

Category		TBR 2 (%)	TBR 1 (%)	TIR (%)	TAR 1 (%)	TAR 2 (%)	LBGI (.)	HBGI (.)	Mean BG (mg/dl)	TDI (U)
Adu.	MDI	2.8 (5.4)	6.8 (8.9)	81.8 (8.4)	11.5 (5.1)	0.3 (1.2)	1.8 (2.3)	2.1 (0.9)	122.0 (13.1)	93.7 (20.6)
	CGM	0.8 (2.1)	2.9 (4.3)	81.4 (5.1)	15.7 (2.7)*	6.0 (3.9)*	1.1 (1.1)	3.7 (1.2)*	129.6 (6.9)	91.2 (20.5)
	Bios.	0.0 (0.0)*	0.0 (0.0)*†	83.4 (3.6)†	16.6 (3.6)*	5.9 (4.9)*	0.1 (0.1)*†	3.8 (1.6)*	137.3 (9.5)*†	87.4 (19.2)*†

Simulation results were analysed for adults (Adu.) after closed-loop simulations of three regulation schemes: Multiple Daily Injections (MDI), a CGM-based AP (CGM), and a biosensor-based AP (Bios.). Case studies 1 and 2 consider a realistic daily glucose intake pattern consisting in three meals (45, 70 and, 80g) and two snacks (20g). Case study 3 considers a challenging daily glucose intake pattern consisting in two meals (100 and 120g) and one snack (20g). No meal announcement is implemented for CGM and Bios. closed-loop schemes. Random errors in carbohydrates counting provided to MDI algorithm are implemented in case studies 2 and 3. The metrics extracted for this comparison are the Time Below Range (TBR) percentage (level 1 and 2), Time In Range (TIR) percentage, Time Above Range (TAR) percentage (level 1 and 2), Low- and High- Blood Glucose Index (LBGI and HBGI) (unitless), mean Blood Glucose (Mean BG) concentration in mg/dl, and Total Daily Insulin (TDI) in units of insulin. All metrics are mean (SD). Symbol $*$ indicates statistical significance ($p > 0.01$) with respect to MDI and symbol † indicates statistical significance ($p > 0.01$) with respect to CGM.

glucose-only sensors for controlling insulin delivery, even with subcutaneous routes. While in vivo experiments are essential in the long term (ongoing work by the authors), we preemptively validate in this paper the working principle of the biosensor in silico.

Simulation results were analysed for adults (Adu.) after closed-loop simulations of three regulation schemes: Multiple Daily Injections (MDI), a CGM-based AP (CGM), and a biosensor-based AP (Bios.). Case studies 1 and 2 consider a realistic daily glucose intake pattern consisting in three meals (45, 70 and, 80g) and two snacks (20g). Case study 3 considers a challenging daily glucose intake pattern consisting in two meals (100 and 120g) and one snack (20g). No mal announcement is implemented for CGM and Bios. closed-loop schemes. Random errors in carbohydrates counting provided to MDI algorithm are implemented in case studies 2 and 3. The metrics extracted for this comparison are the Time Below Range (TBR) percentage (level 1 and 2), Time In Range (TIR) percentage, Time Above Range (TAR) percentage (level 1 and 2), Low- and High- Blood Glucose Index (LBGI and HBGI) (unitless), mean Blood Glucose (Mean BG) concentration in mg/dl, and Total Daily Insulin (TDI) in units of insulin. All metrics are mean (SD). Symbol $*$ indicates statistical significance ($p<0.01$) with respect to MDI and symbol † indicates statistical significance ($p<0.01$) with respect to CGM.

The excellent results in IV/IV simulations validate the use of electrical measurements of islet activity as a means to characterize and exploit the inborn algorithms of pancreatic islets in a BG regulation closed-loop. Indeed, the simulator's T1D cohort was maintained in the normoglycaemic range (70 to 180 mg/dl) for a minimum of 97%, 82%, and 86% of the simulation length (for adults, adolescents, and children respectively) with reduced glycaemia-related risk (assessed with BGI – see Fig. 5B and Table II).

Moreover, the IV/IV configuration also enables a comparison of models presenting different degrees of accuracy in describing the endogenous algorithms. The hysteretic model, providing a better fit to experimental data (see Fig. 4 and Table I), presented slightly better IV/IV results (see Table II) than the static model at the cost of an increased computation time (2% to 4% increase). At the current stage of our research, computational cost is not an issue (as opposed to computation cost in medical devices),

validation in SC/SC configuration was thus conducted using the more accurate hysteretic model.

Healthy pancreatic islets constitutes the core element of our biosensor, therefore the IV/IV results provided a successful proof of concept of its working principle. Subsequently, the SC/SC performance of a Biosensor-AP were assessed and compared to standard treatments (CGM-AP and MDI therapy), which required personalized controllers to better handle the delays induced by the subcutaneous measurement of glucose and the onset of action of subcutaneously-infused insulin in three realistic case studies.

In the first case study, the MDI therapy outperformed closed-loop therapies. This result may come as a surprise considering the well-known superiority of sensor-augmented insulin-pump therapy over MDI demonstrated in real-world clinical trials [37]. However, mathematical modelling implies many simplifications regarding the complexity of the human body and environmental contributions which have to be considered when interpretating these in silico results. The absence of meal anouncement put the closed-loop regulation schemes at a disadvantage, therefore benefitting the non-causal MDI therapy. MDI also benefits from the absence of errors in the patient-provided carbohydrate counting which is unrealistic according to the literature [38]. This point was addressed in case study 2 with a more realistic implementation of the meal anouncement (see Herrero *et al.* [18]) which led to a decrease in MDI performance. For its part, the Biosensor-AP was less efficient than the MDI therapy but still outperformed the CGM-AP with a 4.4% difference in the mean TIR and a lower cumulated glycaemia-related risk (lower LBGI and HBGI, see Table III). The third case study (challenging glucose intake scenario with two large meals and one snack) further emphasized the impact of carbohydrate counting errors on MDI performance. The hypoglyceamic risk increased even more and the mean TIR for MDI therapy decreased below that of the closed-loop schemes.

In a closed-loop system integrating a sensor and a controller, highlighting the sensor's contribution to the whole system's performance is challenging. To address this issue, we assessed the inner regulation capabilities of the biosensor alone with the IV/IV campaign. In addition, the Total Daily Insulin (TDI) indicator revealed the ability of the biosensor to modulate insulin delivery through simulations in SC/SC configuration (with a controller). Using the same controller settings for all case studies, we observed that the Biosensor-AP injected more insulin than the CGM-AP in the first two case studies, whereas in the third one, it injected significantly less insulin than the CGM-AP. Although the same controller tuning methodology was used in both cases, this modulation, induced by the biosensor, enabled the Biosensor-AP to lower the mean BGI of the adult T1D cohort in all case studies.

SC/SC results of adolescents and children are not presented here since our Biosensor-AP could not mitigate the hypoglycemic risk of these patients which therefore presented elevated LBGI values contrasting with good mean TIR results. Analysing the Total Daily Insulin (TDI) injected to these patients, we observed that our methodology tends to be excessively aggressive in the tuning of the derivative action of the PD_{BASAL} controller. Additionally, the meal scenarios represent excessive (and unrealistic) daily glucose intake for young adolescents and children, which makes the controller's task even harder. This issue could be solved by defining weight-dependant meals, a feature not available in the current version 3.2 of the T1DMS. One can also note that a proper validation of the biosensor with multi-meal scenarios would require to model the circadian insulin sensitivity variability observed in real patients. Although it has been studied and published [21], [39], [40], this feature is not yet implemented in the commercial version of the T1DMS.

The MDI therapy and the CGM-AP were rendered more realistic in this work by the introduction of errors in the carbohydrate counting (second case study) and by the presence of measurement noise in the CGM sensor model (even when averaged out over 25 simulations). Our model considers the biosensor as ideal since no parasitic component is implemented. This assumption is relevant considering that measurement noise does not significantly affect performance due to low SP frequency (0-2 Hz). A wearable implementation of our biosensor would however require an osmotic pump coupled with a microfluidic chip to feed the biosensor islets with patient's interstitial fluids. Due to tubing and perfusion safety constraints, the microfluidic setup would certainly induce additional delay in the measurement chain thus degrading closed-loop performance. For reliability purpose, the sensor device would require some ten islets to provide a statistical mean. As the device will be extracorporeal and fed by subcutaneous microdialysis via a 20kDa cut-off membrane, immune attacks are unlikely. Moreover, we currently foresee a sensor life-time of about a week. Finally, as islets are kept in a microfluidic chamber, vascularization is not required. However, continuous monitoring of their electrical activity requires to develop technical solutions to immobilize them in the microfluidic chip.

Finally, a major limitation when using the T1DMS is that only glucose-insulin interactions are modelled, which is perfectly relevant for CGM sensor testing but insufficient to fully assess the performance of our Biosensor-AP. Indeed, its major added value is expected to result from its sensitivity to all nutrients and hormones that participate in the regulation of insulin secretion in a healthy pancreas. However, a glucose-only testing environment, as used here, provides rather an estimation of minimal performance. The biosensor properly captures the modulation of islet responses induced by GLP-1 and adrenaline (see Lebreton *et al.* [11]) which are not implemented in T1DMS, and consequently we hypothesize that accounting for other mediators of insulin would improve the regulation performance and not the opposite.

V. Conclusion

Our work validates the concept of using pancreatic islets algorithms via electrophysiological measurements in a biosensor. Most notably, when simulating the Biosensor-AP, we observed that patient-specific tuning of the controller results in excellent performance with a simple PD_{BASAL} controller. Thus, using the UVA/Padova T1DM Simulator, we demonstrate that our AP is able to regulate the glycaemia of virtual T1D patients as well as a CGM-AP or a MDI therapy, with even better performance under highly challenging glucose intake scenarios.

REFERENCES

[1] D. Rodbard, "Continuous glucose monitoring: A review of successes, challenges, and opportunities," *Diabetes Technol. Ther.*, vol. 18, no. S2, pp. S23–S213, 2016, doi: 10.1089/dia.2015.0417.

[2] B. P. Kovatchev, "Metrics for glycaemic control-from HbA1c to continuous glucose monitoring," *Nature Rev. Endocrinol.*, vol. 13, no. 7, pp. 425–436, 2017, doi: 10.1038/nrendo.2017.3.

[3] A. Basu *et al.*, "Time lag of glucose from intravascular to interstitial compartment in type 1 Diabetes," *J. Diabetes Sci. Technol.*, vol. 9, no. 1, pp. 63–68, 2015, doi: 10.1177/1932296814554797.

[4] H. Thabit and R. Hovorka, "Coming of age: The artificial pancreas for type 1 Diabetes," *Diabetologia*, vol. 59, no. 9, pp. 1795–1805, 2016, doi: 10.1007/s00125-016-4022-4.

[5] J. Fuchs and R. Hovorka, "Closed-loop control in insulin pumps for type-1 diabetes mellitus: safety and efficacy," *Exp. Rev. Med. Devices*, vol. 17, no. 7, pp. 707–720, 2020.

[6] J. H. Youson and A. A. Al-Mahrouki, "Ontogenetic and phylogenetic development of the endocrine pancreas (islet organ) in fishes," *Gen. Comp. Endocrinol.*, vol. 116, no. 3, Dec. 1999, pp. 303–335, doi: 10.1006/gcen.1999.7376.

[7] P. Rorsman and F. M. Ashcroft, "Pancreatic β-cell electrical activity and insulin secretion: Of mice and men," *Physiol. Rev.*, vol. 98, no. 1, pp. 117–214, 2018, doi: 10.1152/physrev.00008.2017.

[8] A. Caicedo, "Paracrine and autocrine interactions in the human islet: More than meets the eye," *Seminars Cell Devlop. Biol.*, vol. 24, no. 1, pp. 11–21, 2013, doi: 10.1016/j.semcdb.2012.09.007.

[9] M. Jaffredo *et al.*, "Dynamic uni- and multicellular patterns encode biphasic activity in pancreatic islets," *Diabetes*, vol. 70, no. 4, pp. 878–888, Apr. 2021.

[10] D. M. Keenan *et al.*, "Logistic model of glucose-regulated C-peptide secretion: Hysteresis pathway disruption in impaired fasting glycemia," *Amer. J. Physiol. Endocrinol. Metab.*, vol. 303, pp. 397–409, 2012, doi: 10.1152/ajpendo.00494.2011.

[11] F. Lebreton *et al.*, "Slow potentials encode intercellular coupling and insulin demand in pancreatic beta cells," *Diabetologia*, vol. 58, no. 6, pp. 1291–1299, 2015, doi: 10.1007/s00125-015-3558-z.

[12] R. Perrier *et al.*, "Bioelectronic organ-based sensor for microfluidic real-time analysis of the demand in insulin," *Biosens. Bioelectron.*, vol. 117, pp. 253–259, 2018, doi: 10.1016/j.bios.2018.06.015.

[13] M. Raoux *et al.*, "Diabetachip: Organ-on-chip for a novel cell-based biosensor in pretransplantation quality control and in treatment of type 1 diabetes," 2014.

[14] R. K. P. Benninger and D. W. Piston, "Cellular communication and heterogeneity in pancreatic islet insulin secretion dynamics," *Trends Endocrinol. Metab.*, vol. 25, no. 8, pp. 399–406, Aug. 2014, doi: 10.1016/j.tem.2014.02.005.

[15] K. Fritzen, L. Heinemann, and O. Schnell, "Modeling of diabetes and its clinical impact," *J. Diabetes Sci. Technol.*, vol. 12, no. 5, pp. 976–984, 2018, doi: 10.1177/1932296818785642.

[16] B. P. Kovatchev *et al.*, "In silico preclinical trials: A proof of concept in closed-loop control of type 1 diabetes," *J. Diabetes Sci. Technol.*, vol. 3, no. 1, pp. 44–55, 2009, doi: 10.1177/193229680900300106.

[17] C. D. Man, R. A. Rizza, and C. Cobelli, "Meal simulation of glucose-insulin system," *IEEE Trans. Biomed. Eng.*, vol. 54, no. 10, pp. 1–33, Oct. 2007.

[18] P. Herrero *et al.*, "A coordinated control strategy for insulin and glucagon delivery in type 1 diabetes," *Comput. Methods Biomech. Biomed. Eng.*, vol. 20, no. 13, pp. 1474–1482, 2017, doi: 10.1080/10255842.2017.1378352.

[19] M. D. Breton *et al.*, "Analysis of the accuracy and performance of a continuous glucose monitoring sensor prototype: An in-silico study using the UVA/PADOVA type 1 diabetes simulator," *J. Diabetes Sci. Technol.*, vol. 11, no. 3, pp. 545–552, 2017, doi: 10.1177/1932296816680633.

[20] C. M. Ramkissoon *et al.*, "Unannounced meals in the artificial pancreas: Detection using continuous glucose monitoring," *Sensors (Switzerland)*, vol. 18, no. 3, pp. 1–18, 2018, doi: 10.3390/s18030884.

[21] R. Visentin *et al.*, "The UVA/Padova type 1 diabetes simulator goes from single meal to single day," *J. Diabetes Sci. Technol.*, vol. 12, no. 2, pp. 273–281, 2018, doi: 10.1177/1932296818757747.

[22] C. Dalla Man *et al.*, "The UVA/PADOVA type 1 diabetes simulator: New features," *J. Diabetes Sci. Technol.*, vol. 8, no. 1, pp. 26–34, 2014, doi: 10.1177/1932296813514502.

[23] A. Pirog *et al.*, "Multimed: An integrated, multi-application platform for the real-time recording and sub-millisecond processing of biosignals," *Sensors (Switzerland)*, vol. 18, no. 7, pp. 1–25, 2018, doi: 10.3390/s18072099.

[24] F. Preisach, "Über die magnetische nachwirkung," *Zeitschrift für Phys.*, vol. 94, no. 5/6, pp. 277–302, May 1935, doi: 10.1007/BF01349418.

[25] V. Janičić *et al.*, "An approach to modeling the hysteresis in ferromagnetic by adaptation of Preisach model," in *Proc. 22nd Telecommun. Forum, TELFOR 2014 - Proc. Pap.*, Nov. 2015, pp. 761–764, doi: 10.1109/TELFOR.2014.7034518.

[26] L. Olçomendy *et al.*, "Tuning of an artificial pancreas controller: An in silico methodology based on clinically-relevant criteria," in *Proc. 42nd Annu. Int. Conf. IEEE Eng. Med. Biol. Soc.*, 2020, [Online]. Available: https://hal.archives-ouvertes.fr/hal-02908200

[27] G. Agiostratidou *et al.*, "Standardizing clinically meaningful outcome measures beyond HbA1c for type 1 diabetes: A consensus report of the American Association of Clinical Endocrinologists, the American Association of Diabetes Educators, the American Diabetes Association, the Endo," *Diabetes Care*, vol. 40, no. 12, pp. 1622–1630, 2017, doi: 10.2337/dc17-1624.

[28] J. R. Petrie *et al.*, "Improving the clinical value and utility of CGM systems: Issues and recommendations: A joint statement of the european association for the study of diabetes and the american diabetes association diabetes technology working group," *Diabetologia*, vol. 60, no. 12. pp. 2319–2328, 2017, doi: 10.1007/s00125-017-4463-4.

[29] T. Danne *et al.*, "International consensus on use of continuous glucose monitoring," *Diabetes Care*, vol. 40, no. 12, pp. 1631–1640, 2017, doi: 10.2337/dc17-1600.

[30] T. Battelino *et al.*, "Clinical targets for continuous glucose monitoring data interpretation: Recommendations from the international consensus on time in range," *Diabetes Care*, vol. 42, no. 8, pp. 1593–1603, 2019, doi: 10.2337/dci19-0028.

[31] B. P. Kovatchev *et al.*, "Quantifying temporal glucose variability in diabetes via continuous glucose monitoring: Mathematical methods and clinical application," *Diabetes Technol. Ther.*, vol. 7, no. 6, pp. 849–862, 2005, doi: 10.1089/dia.2005.7.849.

[32] B. P. Kovatchev *et al.*, "Algorithmic evaluation of metabolic control and risk of severe hypoglycemia in type 1 and type 2 diabetes using self-monitoring blood glucose data," *Diabetes Technol. Ther.*, vol. 5, no. 5, pp. 817–828, 2003, doi: 10.1089/152091503322527021.

[33] R. Oza-Frank *et al.*, "Trends in nutrient intake among adults with diabetes in the United States: 1988-2004," *J. Amer. Diet. Assoc.*, vol. 109, no. 7, pp. 1173–1178, 2009, doi: 10.1016/j.jada.2009.04.007.

[34] M. Breton and B. Kovatchev, "Analysis, modeling, and simulation of the accuracy of continuous glucose sensors," *J. Diabetes Sci. Technol.*, vol. 2, no. 5, pp. 853–862, 2008, doi: 10.1177/193229680800200517.

[35] A. Hill, "The possible effects of the aggregation of the molecules of haemoglobin on its dissociation curves," *J. Physiol.*, vol. 40, pp. 4–7, 1910, Accessed: Mar. 23, 2020. [Online]. Available: https://ci.nii.ac.jp/naid/10020096935/

[36] M. Raoux *et al.*, "Non-invasive long-term and real-time analysis of endocrine cells on micro-electrode arrays," *J. Physiol.*, vol. 590, no. 5, pp. 1085–1091, 2012, doi: 10.1113/jphysiol.2011.220038.

[37] R. M. Bergenstal *et al.*, "Effectiveness of sensor-augmented insulin-pump therapy in type 1 diabetes," *N. Engl. J. Med.*, vol. 363, no. 4, pp. 311–320, Jul. 2010, doi: 10.1056/NEJMoa1002853.

[38] A. S. Brazeau *et al.*, "Carbohydrate counting accuracy and blood glucose variability in adults with type 1 diabetes," *Diabetes Res. Clin. Pract.*, vol. 99, no. 1, pp. 19–23, Jan. 2013, doi: 10.1016/j.diabres.2012.10.024.

[39] R. Visentin *et al.*, "Circadian variability of insulin sensitivity: Physiological input for in silico artificial pancreas," *Diabetes Technol. Ther.*, vol. 17, no. 1, pp. 1–7, 2015, doi: 10.1089/dia.2014.0192.

[40] R. Visentin, C. D. Man, and C. Cobelli, "One-day bayesian cloning of type 1 diabetes subjects: Toward a single-day UVA/Padova type 1 diabetes simulator," *IEEE Trans. Biomed. Eng.*, vol. 63, no. 11, pp. 2416–2424, Nov. 2016, doi: 10.1109/TBME.2016.2535241.